Code-Multiplexing Based One-Way Detect-and-Forward Relaying Schemes for Multiuser UWB MIMO Systems

Antonio A. D'Amico

Abstract—In this paper we consider decode-and-forward one-way relaying schemes for multiuser impulse-radio ultra wideband communications. We assume low-complexity terminals with limited processing capabilities, and a central transceiver unit (i.e. the relay) with a higher computational capacity. All nodes have a single antenna differently from the relay in which multiple antennas may be installed. In order to keep the complexity as low as possible, we concentrate on non-coherent transceiver architectures based on multiuser code-multiplexing transmitted-reference schemes. We propose various relaying systems with different computational complexity and different levels of required channel knowledge. The proposed schemes largely outperform systems without relay in terms of both bit error rate performance and coverage.

I. INTRODUCTION

Multiple antennas at the transmitter and/or at the receiver can be effectively used in UWB systems [1]–[12] to overcome the difficulties due to the strict limitations on the average power spectral density (PSD) of the transmitted signals imposed by regulatory authorities [13], [14]. For a comprehensive survey of UWB multiple-input multiple-output (MIMO) techniques, the reader is referred to [15] and to the articles cited therein.

Relay communications can be used in conjunction with MIMO technology to improve the reliability and coverage of wireless systems [16]. Relaying schemes can be classified according to how the received signals are processed by the relay. In the simplest case, corresponding to the *amplify-and-forward* (AF) protocol, the waveforms at the relay are only filtered before they are retransmitted to the intended destination. Although the AF protocol provides a reasonable trade-off between benefits and practical implementation costs, it is affected by noise propagation mechanisms which limit its performance. In this respect, some improvements can be obtained with *decode-and-forward* (DF) schemes [17]. In this case, the relay first decodes the source message, and then transmits a re-encoded message to the destination. A second distinction can be made between *one-way* and *two-way* relaying systems. The one-way class refers to systems in which four phases are needed to exchange information between source and destination via the relay: Two phases are required to convey data from source to relay and from

relay to destination. Two other phases are needed for data transmission in the reverse direction. On the other hand, in two-way protocols there are only two phases: During the first phase all the terminals act like source nodes, and transmit their information to the relay simultaneously. The information received at the relay is then forwarded to the terminals (which act like destination nodes) in the second phase. Since all the terminals know their own transmitted data, they can remove the self-interference from the received signal provided that the required channel state information is available.

While a relatively intense research effort has been devoted to the optimization of point-to-point (single-hop) MIMO UWB systems, the design of MIMO UWB relay networks has not gained much attention yet. A single-user single-antenna non-coherent UWB relay system is considered in [18], where a two-way DF protocol is proposed and analyzed. The transceiver architecture adopted in [18] is based on the code-multiplexed transmitted-reference scheme proposed in [19]. In [20] space-time codes are designed for high-data rate UWB relay systems. A one-way DF protocol is considered, in which multiple relays simultaneously send their encoded data streams to the destination, after having decoded the message transmitted by the source. Each receiver in the network adopts a Rake-based detection scheme. Single-user UWB relay systems are analyzed in [21]. In particular, a one-way DF protocol is adopted in which the relay is equipped with one or two antennas. Both coherent and non-coherent detectors are considered. The former are based on a selective-Rake architecture while the latter are used with a differential transmitted-reference (DTR) signalling scheme [22], [23]. Non-coherent DTR-based transceivers are also considered in [24]–[26], for single-user single-antenna one-way relaying networks. More specifically, in [25], a two-hop AF protocol is proposed which exploits both the direct path (source-destination) and the relayed link (source-relay-destination). Multiple-hop architectures are analyzed in [24] and [26], in conjunction with AF and DF relaying, respectively. A one-way DF protocol is investigated in [27] where the wireless network contains the source-destination link in addition to the source-relay and relay-destination links. All the nodes of the network are equipped with a single antenna. In order to reduce the receiver complexity, the signalling scheme at both the source and the relay is based on the "time-reversal" technique [28]–[30]. Rake-receivers and time-reversed transmissions (pre-rake filtering) are used in [31] for the design of single-user MIMO UWB one-way relaying systems, with multiple antennas at the

The author is with the Department of Information Engineering, Via Caruso 16, 56100 Pisa, Italy. E-mail:antonio.damico@iet.unipi.it

source and destination nodes, and at the relay. Recently, in [32] post/pre-rake filtering have also been proposed for multiuser two-way schemes, in conjunction with filter-and-forward (FF) or DF relaying protocols. Source and destination nodes have a single antenna whereas multiple antennas are installed at the relay.

Coherent architectures (with Rake/matched filter receivers and/or time-reversed transmissions) have good performance but requires high sampling rates and intensive digital processing [33]. In low data-rate applications, non-coherent schemes based on transmitted reference (TR) systems [19], [22], [34]–[37], or energy detectors (ED) [38]–[40], are preferable in view of their limited complexity and low-power requirements. Nonetheless, very few works have been devoted to the design of *non-coherent multiuser* UWB MIMO relaying systems. In this paper we try to fill this gap. More precisely, we consider a multiuser DF one-way scheme with U pairs of nodes and one relay. Each node of a pair is connected to the other node of that pair via the relay. Following the same line of reasoning as in [32] we consider a network with low-complexity nodes and a central transceiver unit (i.e. the relay) with a higher computational capacity. All nodes have a single antenna while the relay has N_a antennas, with $N_a \geq 1$. In order to keep the complexity as low as possible, we concentrate on the multiuser code-multiplexing transmitted-reference (CM-TR) systems proposed and analyzed in [41], [42]. In particular, we assume that in the uplink (source-relay link) each node transmits following the asynchronous multiuser scheme described in [41, Section II.B]- [42], while in the downlink (relay-destination link) communications take place according to the synchronous scheme in [41, Section II.A]. The detection strategies implemented at the relay *are not a mere extension* of those already proposed in [42] to the case in which the receiver is equipped with multiple-antennas. Actually, we propose and analyze novel detectors characterized by different levels of complexity and/or different levels of required channel knowledge. As for the downlink, we extend the transmission scheme proposed in [41, Section II.A] to the case in which the transmitter (i.e. the relay) has multiple antennas. In doing so, we introduce some weighting factors which can be optimized in order to minimize the maximum bit error rate (BER) among all users under a total power constraint at the relay. The optimization problem is non-convex. We provide a closed-form solution in the single-user case (with an arbitrary number of antennas), and in the single-antenna scenario (with an arbitrary number of users). In the general case, we provide an approximate solution which is very close to the optimal.

The paper is organized as follows. In the next section we describe the system architecture, and we introduce the signal model for uplink transmissions. In Section III we derive several detection strategies at the relay, which are based on energy measurements of the signals received at the various antennas. Downlink transmissions are considered in Section IV. Simulation results are reported in Section V, and conclusions are finally drawn in Section VI.
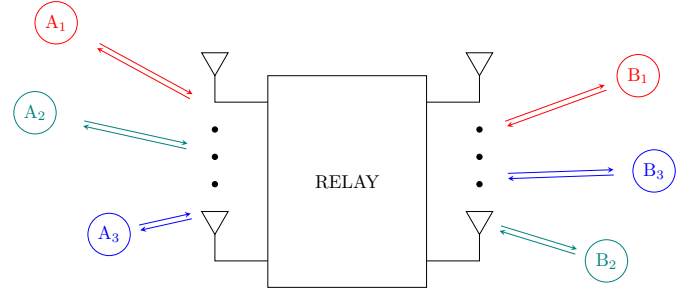

Fig. 1: Block diagram of the relaying scheme for $U = 3$.

II. System Model

The one-way relaying system under investigation is depicted in Fig. 1. We have U pairs of nodes (A_u, B_u), $u = 1, 2, \ldots, U$, and each element of the pair is bi-directionally connected to the other through a relay. The relay is equipped with $N_a \geq 1$ antennas. We ignore the direct link between source and destination nodes, since they are assumed to be at larger distances compared to the source-relay and relay-destination links, with additional path-losses and (possibly) more severe propagation conditions.

The signal generated by the uth transmitter is modelled as

$$s_T^{(u)}(t) = \sum_i \left[\sum_{m=0}^{N_f-1} a_i^{(u)} c_m^{(u)} g(t - t_0^{(u)} - mT_f - iT_s) \right.$$
$$\left. + \sum_{m=0}^{N_f-1} c_m g(t - t_0^{(u)} - mT_f - iT_s) \right] \quad (1)$$

Here, $g(t)$ is the signal pulse or *monocycle*, whose duration is on the order of a nanosecond. Each pulse is confined in a frame of length T_f and there are $N_f = T_s/T_f$ frames in a symbol period. The $a_i^{(u)}$ are data symbols, which are modelled as independent and equally probable random variables ± 1. The quantity $t_0^{(u)}$ represents the offset of the uth transmitter clock with respect to some global time reference. Finally, $\boldsymbol{c}^{(u)} = [c_0^{(u)} c_1^{(u)} \cdots c_{N_f-1}^{(u)}]^T$ and $\boldsymbol{c} = [c_0 c_1 \cdots c_{N_f-1}]^T$ are two code sequences. The former is specific of user u, the latter is common to all users and shapes the reference signal [second line of (1)]. Both $\boldsymbol{c}^{(u)}$ and $\boldsymbol{c}$ have binary components ± 1 and are orthogonal

$$\sum_{m=0}^{N_f-1} c_m^{(u)} c_m = 0 \qquad 1 \leq u \leq U \quad (2)$$

In the sequel $\boldsymbol{c}$ and the $\boldsymbol{c}^{(u)}$ $(u = 1, 2, ..., U)$ are taken from the rows of a Hadamard matrix of size $N_f \times N_f$.

The radio link between the uth transmitter and the nth antenna of the relay is modelled as a multipath channel with impulse response

$$\eta_n^{(u)}(t) = \sum_{\ell=1}^{L_n^{(u)}} \gamma_{n,\ell}^{(u)} \delta(t - \bar{\tau}_{n,\ell}^{(u)}) \quad (3)$$

where $\delta(t)$ is the Dirac delta function, $L_n^{(u)}$ is the number of channel paths, $\gamma_{n,\ell}^{(u)}$ and $\bar{\tau}_{n,\ell}^{(u)}$ are the gain and the delay of

the ℓth path. Without loss of generality we assume $\bar{\tau}_{n,1}^{(u)} < \bar{\tau}_{n,2}^{(u)} \ldots < \bar{\tau}_{n,L_n^{(u)}}^{(u)}$. Thus, $\bar{\tau}_{n,1}^{(u)}$ corresponds to the shortest path and represents the channel propagation delay.

At the nth antenna of the relay, a rectangular filter eliminates the out-of-band noise and collects the users' signals in the single waveform

$$r_n(t) = s_{R,n}(t) + w_n(t) \tag{4}$$

where $w_n(t)$ is Gaussian thermal noise with a flat two-sided power spectral density $N_0/2$ in the filter bandwidth, $s_{R,n}(t)$ is the overall signal component

$$s_{R,n}(t) \triangleq \sum_{u=1}^{U} s_{R,n}^{(u)}(t) \tag{5}$$

while $s_{R,n}^{(u)}(t)$ is the signal from the uth user

$$s_{R,n}^{(u)}(t) = \sum_i \left[\sum_{m=0}^{N_f-1} a_i^{(u)} c_m^{(u)} h_n^{(u)}(t - \tau_n^{(u)} - mT_f - iT_s) \right.$$
$$\left. + \sum_{m=0}^{N_f-1} c_m h_n^{(u)}(t - \tau_n^{(u)} - mT_f - iT_s) \right] \tag{6}$$

In this equation $\tau_n^{(u)}$ is defined as

$$\tau_n^{(u)} \triangleq t_0^{(u)} + \bar{\tau}_{n,1}^{(u)} \tag{7}$$

and $h_n^{(u)}(t - \bar{\tau}_{n,1}^{(u)})$ is the overall response (comprising the receive filter) to a monocycle in the radio link between the uth transmitter and the nth relay antenna. Formally,

$$h_n^{(u)}(t - \bar{\tau}_{n,1}^{(u)}) \triangleq g(t) \otimes \eta_n^{(u)}(t) \otimes g_R(t) \tag{8}$$

where $\otimes$ denotes convolution operation and $g_R(t)$ is the impulse response of the receive filter. We assume that the support of $h_n^{(u)}(t)$ is shorter than T_f. This amounts to saying that the channel response in a frame does not spill over the next frame, i.e. there is no interframe interference (IFI).

Following [42], we model the $\tau_n^{(u)}$, $u = 1, \ldots, U$, and for $n = 1, \ldots, N_a$, as independent random variables (RVs) uniformly distributed over the interval $[0, T_s]$. Although they are not rigorously constant in time as a consequence of the frequency drift of the users' clocks, their variations are assumed to be negligible over several symbol periods. In order to simplify the ensuing discussion, without loss of generality it is assumed $0 \leq \tau_n^{(1)} \leq \cdots \leq \tau_n^{(U)} < T_s$, for $n = 1, 2, \ldots, N_a$. Also, we denote by $\ell_n(u, u')$ and $\Delta_n(u, u')/T_f$, respectively, the integer part and the remainder of $\left| \tau_n^{(u)} - \tau_n^{(u')} \right|/T_f$, i.e.,

$$\left| \tau_n^{(u)} - \tau_n^{(u')} \right| = \ell_n(u, u')T_f + \Delta_n(u, u') \tag{9}$$

with $\ell_n(u, u') \in \{0, 1, \ldots, N_f - 1\}$ and $\Delta_n(u, u') \in [0, T_f)$.

III. DETECTION STRATEGIES AT THE RELAY.

Without loss of generality, we focus on the detection of the data sequence of user #1. In order to reduce the complexity with respect to coherent schemes (which require expensive channel estimation procedures and a Nyquist-rate sampling),

we consider symbol-by-symbol non-coherent detection strategies. In particular, a decision on $a_k^{(1)}$ will be taken on the basis of the following quantities

$$y_{n,m} = \int_{kT_s + mT_f + \tau_n^{(1)}}^{kT_s + (m+1)T_f + \tau_n^{(1)}} r_n^2(t) dt \tag{10}$$

which are computed by integrating the square of the received signal over intervals of length T_f. For the sake of notation, the dependence on index k has not been indicated explicitly, and we have used $y_{n,m}$ instead of $y_{n,m}^{(1)}$. To proceed further, we first determine the conditional probability density function (PDF) of $y_{n,m}$ given the sequences of binary data transmitted by the users. To this purpose, we assume $D = BT_f \gg 1$ with B being the bandwidth of the receive filter. Under the above assumption, $y_{n,m}$ is well approximated by a non-central chi-square (χ^2) random variable with $2D$ degrees of freedom [43] and non-centrality parameter given by

$$\epsilon_{n,m} = \int_{kT_s + mT_f + \tau_n^{(1)}}^{kT_s + (m+1)T_f + \tau_n^{(1)}} s_{R,n}^2(t) dt \tag{11}$$

Accordingly, the PDF of $y_{n,m}$ reads

$$f_{NC}(y_{n,m}; \epsilon_{n,m}) = \frac{1}{N_0} \left(\frac{y_{n,m}}{\epsilon_{n,m}} \right)^{\frac{D-1}{2}} \exp \left(-\frac{y_{n,m} + \epsilon_{n,m}}{N_0} \right)$$
$$\times I_{D-1} \left(\frac{\sqrt{\epsilon_{n,m} y_{n,m}}}{N_0/2} \right) \tag{12}$$

where $I_{D-1}(x)$ is the modified Bessel function of order $D-1$. Taking (6) into account and replacing (5) into (11) yields

$$\epsilon_{n,m} = \int_0^{T_f} \left[(a_k^{(1)} c_m^{(1)} + c_m) h_n^{(1)}(t) + \xi_n(t) \right]^2 dt \tag{13}$$

where

$$\xi_n(t) = \sum_{u=2}^{U} \left[\left(a_{\kappa_1^u}^{(u)} c_{\mu_1^u}^{(u)} + c_{\mu_1^u} \right) h_n^{(u)}(t + T_f - \Delta_n(1, u)) \right.$$
$$\left. + \left(a_{\kappa_2^u}^{(u)} c_{\mu_2^u}^{(u)} + c_{\mu_2^u} \right) h_n^{(u)}(t - \Delta_n(1, u)) \right] \tag{14}$$

with

$$\kappa_1^u = \begin{cases} k-1 & \text{for } 0 \leq m \leq \ell_n(1, u) \\ k & \text{for } \ell_n(1, u) + 1 \leq m \leq N_f - 1 \end{cases}$$

$$\kappa_2^u = \begin{cases} \kappa_1^u + 1 & \text{for } m = \ell_n(1, u) - 1 \\ \kappa_1^u & \text{otherwise} \end{cases} \tag{15}$$

$$\mu_1^u = \text{mod}_{N_f}(m - \ell_n(1, u) - 1)$$
$$\mu_2^u = \text{mod}_{N_f}(\mu_1^u + 1) \tag{16}$$

Parameters $\ell_n(1, u)$ and $\Delta_n(1, u)$ in (14)–(16) are defined in (9). Now, let the channel correlation coefficient

$\rho_n(u, u'; \vartheta_1, \vartheta_2)$ be defined by

$$\rho_n(u, u'; \vartheta_1, \vartheta_2) = \int_0^{T_f} h_n^{(u)}(t - \vartheta_1) h_n^{(u')}(t - \vartheta_2) dt \quad (17)$$

Expanding the square in the integrand of (13), after straightforward calculations one gets:

$$
\begin{aligned}
\epsilon_{n,m} &= (a_k^{(1)} c_m^{(1)} + c_m)^2 \rho_n(1,1;0,0) \\
&+ 2(a_k^{(1)} c_m^{(1)} + c_m) \sum_{u=2}^{U} \zeta_{1,u} \rho_n\big(1, u; 0, \Delta_n(1,u) - T_f\big) \\
&+ 2(a_k^{(1)} c_m^{(1)} + c_m) \sum_{u=2}^{U} \zeta_{2,u} \rho_n\big(1, u; 0, \Delta_n(1,u)\big) \\
&+ \sum_{u=2}^{U} \sum_{v=2}^{U} \zeta_{1,u} \zeta_{1,v} \rho_n\big(u, v; \Delta_n(1,u) - T_f, \Delta_n(1,v) - T_f\big) \\
&+ \sum_{u=2}^{U} \sum_{v=2}^{U} \zeta_{2,u} \zeta_{2,v} \rho_n\big(u, v; \Delta_n(1,u), \Delta_n(1,v)\big) \\
&+ 2 \sum_{u=2}^{U} \sum_{v=2}^{U} \zeta_{1,u} \zeta_{2,v} \rho_n\big(u, v; \Delta_n(1,u) - T_f, \Delta_n(1,v)\big)
\end{aligned}
\quad (18)
$$

where

$$\zeta_{1,u} = a_{\kappa_1^u}^{(u)} c_{\mu_1^u}^{(u)} + c_{\mu_1^u} \quad \zeta_{2,u} = a_{\kappa_2^u}^{(u)} c_{\mu_2^u}^{(u)} + c_{\mu_2^u} \quad (19)$$

Notice that $\rho_n(1,1;0,0)$ in the first line of (18) is the energy of $h_n^{(1)}(t)$.

To proceed further, let $\boldsymbol{y}_n^T = [y_{n,0} \, y_{n,1} \, \cdots \, y_{n,N_f-1}]$ denote the vector collecting the quantities $y_{n,m}$ computed at the nth antenna over N_f frames, and let $\boldsymbol{y} = [\boldsymbol{y}_1^T \, \boldsymbol{y}_2^T \cdots \boldsymbol{y}_{N_a}^T]^T$ be the vector obtained by considering all the antennas. Assuming that y_{n_1,m_1} and y_{n_2,m_2} are statistically independent for $n_1 \neq n_2$ or $m_1 \neq m_2$, the PDF of $\boldsymbol{y}$ reads

$$f(\boldsymbol{y}; \boldsymbol{a}, a_k^{(1)}) = \prod_{n=1}^{N_a} \prod_{m=0}^{N_f-1} f_{NC}(y_{n,m}; \epsilon_{n,m}) \quad (20)$$

where its dependence on $\boldsymbol{a} = [a_{k-1}^{(2)}, a_k^{(2)}, \ldots, a_{k-1}^{(U)}, a_k^{(U)}]$ and $a_k^{(1)}$ has been indicated explicitly. A decision about $a_k^{(1)}$ can be taken through a likelihood ratio test. To be specific, let $f(\boldsymbol{y}; a_k^{(1)})$ denote the conditional probability density function of $\boldsymbol{y}$ given $a_k^{(1)}$, which is obtained by averaging (20) with respect to the distribution of $\boldsymbol{a}$. Denoting by $\widetilde{\boldsymbol{a}}_i$ the generic value of $\boldsymbol{a}$, $f(\boldsymbol{y}; a_k^{(1)})$ then reads

$$f(\boldsymbol{y}; a_k^{(1)}) = \frac{1}{N_H} \sum_{i=0}^{N_H-1} f(\boldsymbol{y}; a_k^{(1)}, \widetilde{\boldsymbol{a}}_i) \quad (21)$$

where $N_H = 2^{2(U-1)}$ is the total number of values of $\boldsymbol{a}$. Taking (20) into account, yields

$$f(\boldsymbol{y}; a_k^{(1)}) = \frac{1}{N_H} \sum_{i=0}^{N_H-1} \left[\prod_{n=1}^{N_a} \prod_{m=0}^{N_f-1} f_{NC}\left(y_{n,m}; \epsilon_{n,m}^{(i)}(a_k^{(1)})\right) \right] \quad (22)$$

where $\epsilon_{n,m}^{(i)}(a_k^{(1)})$ is the value of the non-centrality parameter [as given by (11) or, equivalently, by (18)] corresponding to $\widetilde{\boldsymbol{a}}_i$. The dependence of $\epsilon_{n,m}^{(i)}$ on $a_k^{(1)}$ has been indicated explicitly. Based on (22), the likelihood ratio takes the form

$$\Lambda = \frac{f(\boldsymbol{y}; -1)}{f(\boldsymbol{y}; +1)} = \frac{\sum_{i=0}^{N_H-1} \left[\prod_{n=1}^{N_a} \prod_{m=0}^{N_f-1} f_{NC}\left(y_{n,m}; \epsilon_{n,m}^{(i)}(-1)\right) \right]}{\sum_{i=0}^{N_H-1} \left[\prod_{n=1}^{N_a} \prod_{m=0}^{N_f-1} f_{NC}\left(y_{n,m}; \epsilon_{n,m}^{(i)}(+1)\right) \right]} \quad (23)$$

whereas the decision rule becomes

$$\widehat{a}_k^{(1)} = \begin{cases} -1 & \text{for } \Lambda > 1, \\ +1 & \text{otherwise.} \end{cases} \quad (24)$$

Notice that (23)–(24) represents the minimum error probability decision strategy for the class of all the detectors based on the observation of $\boldsymbol{y}$. In practical applications, the implementation of this strategy could be computationally too expensive as it requires the calculation of $2N_H$ values of $f(\boldsymbol{y}; a_k^{(1)}, \boldsymbol{a})$ in (21), namely N_H for $a_k^{(1)} = -1$ and N_H for $a_k^{(1)} = +1$. In order to reduce the computational complexity some approximations are in order. As a first step we get rid of the Bessel functions. Based on the results in [40, Appendix], for $D \gg 1$ it is found that $f(\boldsymbol{y}; a_k^{(1)}, \widetilde{\boldsymbol{a}}_i)$ can be approximated as follows

$$
\begin{aligned}
f(\boldsymbol{y}; a_k^{(1)}, \widetilde{\boldsymbol{a}}_i) &= \prod_{n=1}^{N_a} \prod_{m=0}^{N_f-1} f_{NC}\left(y_{n,m}; \epsilon_{n,m}^{(i)}(a_k^{(1)})\right) \\
&\approx A(\boldsymbol{y}) \left[\frac{\exp\left(\sum_{n=1}^{N_a} \sum_{m=0}^{N_f-1} \sqrt{\frac{\epsilon_{n,m}^{(i)}(a_k^{(1)}) y_{n,m}}{N_0^2 D^2} + 1} - \frac{\epsilon_{n,m}^{(i)}(a_k^{(1)})}{2 N_0 D} \right)}{\prod_{n=1}^{N_a} \prod_{m=0}^{N_f-1} \left(1 + \sqrt{\frac{\epsilon_{n,m}^{(i)}(a_k^{(1)}) y_{n,m}}{N_0^2 D^2} + 1} \right)} \right]^D
\end{aligned}
\quad (25)
$$

where $A(\boldsymbol{y})$ is independent of both $a_k^{(1)}$ and $\widetilde{\boldsymbol{a}}_i$. As a result, after dropping the irrelevant factor $A(\boldsymbol{y})/N_H$, (22) becomes

$$f(\boldsymbol{y}; a_k^{(1)}) \approx \sum_{i=0}^{N_H-1} \left[g_i(\boldsymbol{y}; a_k^{(1)}) \right]^D \quad (26)$$

with

$$g_i(\boldsymbol{y}; a_k^{(1)}) = \frac{\exp\left(\sum_{n=1}^{N_a} \sum_{m=0}^{N_f-1} \sqrt{\frac{\epsilon_{n,m}^{(i)}(a_k^{(1)}) y_{n,m}}{N_0^2 D^2} + 1} - \frac{\epsilon_{n,m}^{(i)}(a_k^{(1)})}{2 N_0 D} \right)}{\prod_{n=1}^{N_a} \prod_{m=0}^{N_f-1} \left(1 + \sqrt{\frac{\epsilon_{n,m}^{(i)}(a_k^{(1)}) y_{n,m}}{N_0^2 D^2} + 1} \right)}$$

The computational advantage of (26) with respect to (22) is evident, since the former does not require the calculation of Bessel functions, differently from the latter.

As a second step, we retain only the maximum term in the summation in (26), and we approximate $f(\boldsymbol{y}; a_k^{(1)})$ as follows

$$f(\boldsymbol{y}; a_k^{(1)}) \approx \left[g(\boldsymbol{y}; a_k^{(1)}) \right]^D \quad (27)$$

with

$$g(\boldsymbol{y}; a_k^{(1)}) = \max_{i=0,\ldots,N_H-1} g_i(\boldsymbol{y}; a_k^{(1)}) \quad (28)$$

We expect such an approximation to be good at high signal-to-noise ratios. Based on (27), the decision rule then reads

$$\widehat{a}_k^{(1)} = \begin{cases} -1 & \text{for } \Lambda_{\text{app}} > 1, \\ +1 & \text{otherwise.} \end{cases} \qquad (29)$$

where

$$\Lambda_{\text{app}} = \frac{g(\boldsymbol{y}; -1)}{g(\boldsymbol{y}; +1)} \qquad (30)$$

Notice that, in computing Λ_{app}, the calculation of the Dth power of $g(\boldsymbol{y}; a_k^{(1)})$ is not required. This is the main advantage of using (27) instead of (26).

Implementing the detection strategies (24) and (29) requires the computation of the non-centrality parameters $\epsilon_{n,m}^{(i)}(a_k^{(1)})$, $i = 0, 1, \ldots, N_H - 1$. In its turn, calculation of $\epsilon_{n,m}^{(i)}(a_k^{(1)})$ requires knowledge of all the channel correlation coefficients $\rho_n(u, u'; \vartheta_1, \vartheta_2)$ that appear in (18). Simplified detectors come from approximating the non-centrality parameter $\epsilon_{n,m}$ in (18) by neglecting the channel correlation coefficients involving two different users, i.e., $\rho_n(u, u'; \vartheta_1, \vartheta_2)$ with $u \neq u'$. In so doing one gets

$$\begin{aligned} \epsilon_{n,m} \approx & \left(a_k^{(1)} c_m^{(1)} + c_m\right)^2 \rho_n(1, 1; 0, 0) \\ & + \sum_{u=2}^{U} \zeta_{1,u}^2 \rho_n\big(u, u; \Delta_n(1, u) - T_f, \Delta_n(1, u) - T_f\big) \\ & + \sum_{u=2}^{U} \zeta_{2,u}^2 \rho_n\big(u, u; \Delta_n(1, u), \Delta_n(1, u)\big) \end{aligned}$$

$$(31)$$

where we have used the fact that

$$\rho_n\big(u, u; \Delta_n(1, u) - T_f, \Delta_n(1, u)\big) = 0,$$

which results from assuming the duration of $h_n^{(u)}(t)$ to be no longer than T_f (no IFI assumption). Observe that $\rho_n\big(u, u; \Delta_n(1, u), \Delta_n(1, u)\big)$ and $\rho_n\big(u, u; \Delta_n(1, u) - T_f, \Delta_n(1, u) - T_f\big)$ in (31) are the energies of $h_n^{(u)}(t)$ in the intervals $[0, T_f - \Delta_n(1, u))$ and $[T_f - \Delta_n(1, u), T_f)$, respectively. Both the detection strategies (24) and (29) can be used in conjunction with the approximate values of $\epsilon_{n,m}$ given by (31). *The detectors obtained in this way have the same computational complexity of those using* (18) *but require less information about the propagation channels.*

The most significant simplification comes from neglecting the presence of the interfering users, just as done in [42]. In this case, the effects of the other users are not taken into account, and the task of rejecting the multiple-access interference (MAI) is only left to the cross-correlation properties of the users' codes. This amounts to approximate $\epsilon_{n,m}$ as

$$\epsilon_{n,m} \approx \left(a_k^{(1)} c_m^{(1)} + c_m\right)^2 \mathcal{E}_n^{(1)} \qquad (32)$$

where $\mathcal{E}_n^{(1)} = \rho_n(1, 1; 0, 0)$ is the energy of $h_n^{(1)}(t)$. In this case, following the approach used in [40] it can be shown that, at low signal-to-noise ratios, the likelihood ratio (23) can be approximated with Λ' given by

$$\Lambda' = \exp\left\{ \sum_{n=1}^{N_a} \sum_{m=0}^{N_f-1} \left(-4 c_m^{(1)} c_m\right) \mathcal{E}_n^{(1)} \cdot \left[1 - \frac{y_{n,m}}{(D-1)N_0}\right] \right\}$$

TABLE I: Detection Strategies at the Relay.

Algorithm	Decision statistic	Decision rule	Non-centrality parameters
OD-CCK	Eq. (23)	Eq. (24)	Eq. (18)
OD-PCK	Eq. (23)	Eq. (24)	Eq. (31)
AOD-CCK	Eq. (30)	Eq. (29)	Eq. (18)
AOD-PCK	Eq. (30)	Eq. (29)	Eq. (31)
DMD-CEK	Eq. (34)	Eq. (35)	Eq. (32)
DMD-NEK	Eq. (36)	Eq. (37)	——

In view of the orthogonality condition (2), the above expression reduces to

$$\Lambda' = \exp\left\{ \frac{4}{N_0 D} \sum_{n=1}^{N_a} \mathcal{E}_n^{(1)} \sum_{m=0}^{N_f-1} c_m^{(1)} c_m y_{n,m} \right\} \qquad (33)$$

Setting

$$\lambda' = \sum_{n=1}^{N_a} \mathcal{E}_n^{(1)} \sum_{m=0}^{N_f-1} c_m^{(1)} c_m y_{n,m} \qquad (34)$$

the decision rule reads

$$\widehat{a}_k^{(1)} = \begin{cases} -1 & \text{if } \lambda' < 0, \\ +1 & \text{otherwise.} \end{cases} \qquad (35)$$

It is worth noticing that (34)-(35) are nothing but an extension of the detector proposed in [42] to the case in which the receiver is equipped with multiple antennas. Eq. (34) simply states that, in the multiple antennas scenario, the decision statistic is a weighted linear combination of the single-antenna decision statistic $\sum_{m=0}^{N_f-1} c_m^{(1)} c_m y_{n,m}$, the weights being the energies $\mathcal{E}_n^{(1)}$. An even simpler decision strategy, which does not require any channel knowledge, can be implemented by dropping the weighting factors in (34). This yields

$$\lambda'' = \sum_{n=1}^{N_a} \sum_{m=0}^{N_f-1} c_m^{(1)} c_m y_{n,m} \qquad (36)$$

and

$$\widehat{a}_k^{(1)} = \begin{cases} -1 & \text{if } \lambda'' < 0, \\ +1 & \text{otherwise.} \end{cases} \qquad (37)$$

A summary of the detection strategies proposed for the source-relay links are provided in Table I, in which acronyms have the following meanings: *i)* OD-CCK stands for Optimum Detector with Complete Correlations Knowledge; *ii)* OD-PCK for Optimum Detector with Partial Correlations Knowledge; *iii)* AOD-CCK for Approximate Optimum Detector with Complete Correlations Knowledge; *iv)* AOD-PCK for Approximate Optimum Detector with Partial Correlations Knowledge; *v)* DMD-CEK for D'Amico-Mengali Detector with Complete Energy Knowledge; *vi)* DMD-NEK for D'Amico-Mengali Detector with No Energy Knowledge.

IV. DOWNLINK TRANSMISSION.

For the transmission from the relay to the destination nodes, we adopt the communication scheme for the downlink channel of the multi-user system described in [41, Section II.A]. The information rate from the relay is $1/T_s$ bit/s per user, and the

signal transmitted from the nth antenna is given by

$$s_{T,n}(t) = \sum_i \left[\sum_{u=1}^{U} \beta_{u,n} \sum_{m=0}^{N_f-1} a_i^{(u)} d_m^{(u)} g(t - mT_f - iT_s) \right.$$
$$\left. + \beta_{0,n} \sum_{m=0}^{N_f-1} d_m g(t - mT_f - iT_s) \right] \quad (38)$$

where $a_i^{(u)}$ is ith symbol for the uth user, $g(t)$ is the downlink pulse which is assumed the same as the uplink pulse, for simplicity, $\{d_m^{(u)}\}_{m=0}^{N_f-1}$ and $\{d_m\}_{m=0}^{N_f-1}$ are the downlink codes for the uth user and the reference signal (which is shared by all users), respectively. The elements of $\{d_m^{(u)}\}_{m=0}^{N_f-1}$ and $\{d_m\}_{m=0}^{N_f-1}$ are binary variables taking values in the set $\{\pm 1\}$, and satisfy the orthogonality conditions

$$\sum_{m=0}^{N_f-1} d_m^{(u)} d_m^{(u')} = N_f \delta_K[u - u'] \qquad u, u' = 1, 2, \ldots, U \quad (39)$$

$$\sum_{m=0}^{N_f-1} d_m^{(u)} d_m = 0 \qquad u = 1, 2, \ldots, U \quad (40)$$

where $\delta_K[j]$ is the Kronecker delta. The real parameters $\beta_{u,n}$, $u = 0, 1, \ldots, U$ are weighting factors that can be properly adjusted in order to optimize the system performance, as described in Section IV-A.

Analogously to the uplink scenario, the radio link (RL) between the nth antenna of the relay and the uth receiver (henceforth referred to as $\mathrm{RL}_{n,u}$) is modelled as a multipath channel with impulse response

$$\eta_n^{(u)}(t) = \sum_{\ell=1}^{L_n^{(u)}} \gamma_{n,\ell}^{(u)} \delta(t - \bar{\tau}_{n,\ell}^{(u)}) \quad (41)$$

where we have used exactly the same notation as in (3) in order not to introduce unnecessary complications.

At the uth destination node, a rectangular front-end filter eliminates the out-of-band noise. Denoting by $h_n^{(u)}(t)$ the overall response (comprising the receive filter) of $\mathrm{RL}_{n,u}$ to a single pulse $g(t)$, the received signal takes the form

$$r^{(u)}(t) = s_R^{(u)}(t) + w^{(u)}(t) \quad (42)$$

where

$$s_R^{(u)}(t) = \sum_i \left[\sum_{v=1}^{U} \sum_{m=0}^{N_f-1} a_i^{(v)} d_m^{(v)} p_v^{(u)}(t - \tau^{(u)} - mT_f - iT_s) \right.$$
$$\left. + \sum_{m=0}^{N_f-1} d_m q^{(u)}(t - \tau^{(u)} - mT_f - iT_s) \right] \quad (43)$$

with

$$p_v^{(u)}(t) = \sum_{n=1}^{N_a} \beta_{v,n} h_n^{(u)}(t + \tau^{(u)}), \quad (44)$$

$$q^{(u)}(t) = \sum_{n=1}^{N_a} \beta_{0,n} h_n^{(u)}(t + \tau^{(u)}), \quad (45)$$

and

$$\tau^{(u)} = \min_{n=1,\ldots,N_a} \min_{\ell=1,\ldots,L_n^{(u)}} \left\{ \bar{\tau}_{n,\ell}^{(u)} \right\} \quad (46)$$

Henceforth, the duration of $p_v^{(u)}(t)$ and $q^{(u)}(t)$ is assumed shorter than T_f, meaning that no IFI occurs. Finally, the noise term $w^{(u)}(t)$ in (42) has a flat power spectral density (PSD) $N_0/2$ in the receive filter bandwidth.

In order to keep the processing complexity at the receiver at a low level, the detection of symbol $a_k^{(u)}$ proceeds as indicated in [41], and is based on the following statistic:

$$z_k^{(u)} = \sum_{m=0}^{N_f-1} d_m^{(u)} d_m \int_{kT_s+mT_f+\tau^{(u)}}^{kT_s+(m+1)T_f+\tau^{(u)}} \left[r^{(u)}(t) \right]^2 dt \quad (47)$$

The decision rule then reads

$$\hat{a}_k^{(u)} = \begin{cases} -1 & \text{if } z_k^{(u)} < 0, \\ +1 & \text{otherwise.} \end{cases} \quad (48)$$

A. Optimization of downlink performance

The downlink performance, in terms of bit error rate (BER), depends on the set of parameters $\mathcal{B} = \{\beta_{u,n}; \ n = 1, \ldots, N_a, \quad u = 0, \ldots, U\}$. In order to optimize the $\beta_{u,n}$, we need to find the dependence of BER_u, for $u = 1, \ldots, U$, on the elements of $\mathcal{B}$. As a first step, we replace (42)–(43) into (47) and we write $z_k^{(u)}$ as the sum of three terms, corresponding to the interactions signal$\times$signal, signal$\times$noise and noise$\times$noise in the square of $r^{(u)}(t)$ (see [41, Eq. (10)]):

$$z_k^{(u)} = z_{k,S\times S}^{(u)} + z_{k,S\times N}^{(u)} + z_{k,N\times N}^{(u)} \quad (49)$$

where

$$z_{k,S\times S}^{(u)} = 2N_f a_k^{(u)} \int_0^{T_f} p_u^{(u)}(t) q^{(u)}(t) dt$$
$$+ \underbrace{\sum_{\substack{v=1 \\ v\neq u}}^{U} \sum_{\substack{v'=1 \\ v'\neq u}}^{U} \left[\sum_{m=0}^{N_f-1} d_m^{(u)} d_m^{(v)} d_m^{(v')} d_m \right] a_k^{(v)} a_k^{(v')} \int_0^{T_f} p_v^{(u)}(t) p_{v'}^{(u)}(t) dt}_{\text{MAI}}$$
$$(50)$$

$$z_{k,S\times N}^{(u)} = 2 \sum_{m=0}^{N_f-1} d_m^{(u)} \int_0^{T_f} q^{(u)}(t) w^{(u)}(t + \theta_{m,k}^{(u)}) dt$$
$$+ 2 \sum_{v=1}^{U} a_k^{(v)} \sum_{m=0}^{N_f-1} d_m^{(u)} d_m^{(v)} d_m \int_0^{T_f} p_v^{(u)}(t) w^{(u)}(t + \theta_{m,k}^{(u)}) dt$$
$$(51)$$

$$z_{k,N\times N}^{(u)} = \sum_{m=0}^{N_f-1} d_m^{(u)} d_m \int_0^{T_f} \left[w^{(u)}(t + \theta_{m,k}^{(u)}) \right]^2 dt \quad (52)$$

with

$$\theta_{m,k}^{(u)} = \tau^{(u)} + mT_f + kT_s$$

Equation (50) expresses $z_{k,S\times S}^{(u)}$ as the sum of a useful

term (proportional to $a_k^{(u)}$) plus an interfering term due to the multiple access. The latter vanishes if the code sequences meet the further condition [in addition to (39)-(40)]

$$\sum_{m=0}^{N_f-1} d_m^{(u)} d_m^{(v)} d_m^{(v')} d_m = 0 \quad u, v, v' = 1, 2, \ldots, U \quad (53)$$

In [41] it is shown that this goal can be achieved if N_f is a power of 2 and the code sequences are chosen from the rows of an $N_f \times N_f$ Hadamard matrix built with the Sylvester method. Actually, it can be shown that up to $N_f/2 + 1$ rows of such a matrix do satisfy (53). In particular, if the common sequence $\boldsymbol{d} = [d_0\, d_1\, \ldots\, d_{N_f-1}]^T$ is chosen among the first $N_f/2$ rows, then the remaining U sequences can be arbitrarily taken from the last $N_f/2$ rows. As a total of $U+1$ sequences are required, the interfering term in (50) can be eliminated provided that $U \leq N_f/2$. Henceforth, we assume that (53) is satisfied so that $z_k^{(u)}$ reduces to

$$z_k^{(u)} = 2N_f a_k^{(u)} \int_0^{T_f} p_u^{(u)}(t) q^{(u)}(t) dt + \nu_k^{(u)} \quad (54)$$

where $\nu_k^{(u)} = z_{k,S\times N}^{(u)} + z_{k,N\times N}^{(u)}$. In order to proceed further in the computation of BER_u, we are now forced to make some approximations. To be specific, we model the noise term $\nu_k^{(u)}$ as a Gaussian random variable (RV) just as in [41], where it has been shown that such a theoretical model is in very good agreement with simulation results. Taking (51)-(52) into account, it is easily verified that $\nu_k^{(u)}$ is a zero-mean RV. Also, assuming that $BT_f \gg 1$, with B being the bandwidth of the receive filter, the conditional variance of $\nu_k^{(u)}$, for given values of the information symbols $\{a_k^{(v)}\}_{v=1}^U$, can be approximated as

$$\sigma_{\nu,u}^2 \approx 4N_f \sum_{v=1}^U \int_0^{T_f}\int_0^{T_f} p_v^{(u)}(t_1)p_v^{(u)}(t_2)R_w(t_1-t_2)dt_1 dt_2$$
$$+ 4N_f \int_0^{T_f}\int_0^{T_f} q^{(u)}(t_1)q^{(u)}(t_2)R_w(t_1-t_2)dt_1 dt_2$$
$$+ 2N_f \int_0^{T_f}\int_0^{T_f} R_w^2(t_1-t_2)dt_1 dt_2 \quad (55)$$

where $R_w(\tau)$ is the auto-correlation function of $w^{(u)}(t)$. It is worth noting that $\sigma_{\nu,u}^2$ does not depend on the set $\{a_k^{(v)}\}_{v=1}^U$. The expression (55) can be further simplified when $g_R(t)$ is a rectangular filter. In this case (which will be considered later in the Simulation Results section) one gets

$$\sigma_{\nu,u}^2 \approx 2N_f N_0 \sum_{v=1}^U \int_0^{T_f} \left[p_v^{(u)}(t)\right]^2 dt$$
$$+ 2N_f N_0 \int_0^{T_f} \left[q^{(u)}(t)\right]^2 dt + N_f T_f B N_0^2 \quad (56)$$

Taking (54) and (56) into account, the bit error rate for the uth user reads

$$\mathrm{BER}_u = Q\left(\sqrt{\frac{4N_f(\boldsymbol{\beta}_u^T \mathbf{H}_u \boldsymbol{\beta}_0)^2}{2N_0 \sum_{v=0}^U \boldsymbol{\beta}_v^T \mathbf{H}_u \boldsymbol{\beta}_v + T_f B N_0^2}}\right) \quad (57)$$

where the element (i,j) of the $N_a \times N_a$ symmetric matrix $\mathbf{H}_u$ is given by

$$[\mathbf{H}_u]_{i,j} = \int_0^{T_f} h_i^{(u)}(t+\tau^{(u)})h_j^{(u)}(t+\tau^{(u)})dt, \quad (58)$$

$\boldsymbol{\beta}_v = [\beta_{v,1}\beta_{v,2}\cdots\beta_{v,N_a}]^T$ is the real column-vector collecting the weighting factors for user v, with $v = 1, \ldots, U$, and $\boldsymbol{\beta}_0 = [\beta_{0,1}\beta_{0,2}\cdots\beta_{0,N_a}]^T$.

The simplest design of the vectors $\boldsymbol{\beta}_u$ is that corresponding to equal values of the weighting factors (Uniform Power Allocation, UPA), namely $\beta_{u,n} = \beta$, for $u = 0, \ldots, U$, and $n = 1, \ldots, N_a$, just as it has been done in the single-antenna scenario analyzed in [41]. In the UPA case, (57) reduces to

$$\mathrm{BER}_{u,UPA} = Q\left(\sqrt{\frac{[2U/(U+1)]^2}{2U \cdot \mathrm{SNR}_{u,UPA}^{-1} + N_f T_f B \cdot \mathrm{SNR}_{u,UPA}^{-2}}}\right) \quad (59)$$

where

$$\mathrm{SNR}_{u,UPA} = \frac{N_f(U+1)\beta^2}{U} \cdot \frac{\mathbf{1}^T \mathbf{H}_u \mathbf{1}}{N_0} \quad (60)$$

is the ratio between the *received* energy per bit and N_0 at uth destination node with a uniform power allocation.

In this paper we consider a different design criterion based on the minimization of the maximum BER among all users under a total power constraint at the relay [44]. For this purpose, we first compute the mean power P_s of the transmitted signal over a symbol interval T_s. Taking (38) into account, it is easily found

$$P_s = P_g \sum_{n=1}^{N_a}\sum_{u=0}^U \beta_{u,n}^2 = P_g \sum_{u=0}^U \|\boldsymbol{\beta}_u\|^2 \quad (61)$$

where $P_g = [\int g^2(t)dt]/T_f$ is the mean power of $g(t)$ over a frame interval, and $\|\cdot\|$ denotes the norm of the enclosed vector. It is seen that the right-hand side of (61) is independent of the particular symbol interval, as expected, and hence constraining the mean transmitted power amounts to constraining P_s. In turn, this amounts to constraining $\sum_{u=0}^U \|\boldsymbol{\beta}_u\|^2$. Accordingly, we consider the following optimization problem:

$$\mathcal{P}: \quad \min_{\boldsymbol{\beta}_0,\ldots,\boldsymbol{\beta}_U} \max_u \quad \mathrm{BER}_u$$
$$\text{subject to} \quad \sum_{u=0}^U \|\boldsymbol{\beta}_u\|^2 \leq P \quad (62)$$

with BER_u given by (57). Due to the monotonic properties of function Q, (62) is equivalent to

$$\mathcal{P}: \quad \max_{\boldsymbol{\beta}_0,\ldots,\boldsymbol{\beta}_U} \min_u \quad \frac{(\boldsymbol{\beta}_u^T \mathbf{H}_u \boldsymbol{\beta}_0)^2}{2N_0 \left(\sum_{v=0}^U \boldsymbol{\beta}_v^T \mathbf{H}_u \boldsymbol{\beta}_v \right) + T_f B N_0^2}$$

$$\text{subject to} \quad \sum_{u=0}^U \|\boldsymbol{\beta}_u\|^2 \le P \tag{63}$$

which can also be written as

$$\mathcal{P}: \quad \max \quad t$$

$$\text{subject to} \quad t \le \frac{(\boldsymbol{\beta}_u^T \mathbf{H}_u \boldsymbol{\beta}_0)^2}{2N_0 \left(\sum_{v=0}^U \boldsymbol{\beta}_v^T \mathbf{H}_u \boldsymbol{\beta}_v \right) + T_f B N_0^2}$$

$$u = 1, \ldots, U$$

$$\sum_{u=0}^U \|\boldsymbol{\beta}_u\|^2 \le P \tag{64}$$

Problem $\mathcal{P}$ has a closed form solution in the following two cases:

1) single-user scenario (i.e. $U = 1$) with an arbitrary number of antennas N_a;
2) single-antenna scenario (i.e. $N_a = 1$) with an arbitrary number of destination nodes U.

In the first case it can be shown (we omit the proof for limitations of space) that the optimal weights $\hat{\boldsymbol{\beta}}_0$ and $\hat{\boldsymbol{\beta}}_1$ are given by

$$\hat{\boldsymbol{\beta}}_0 = \hat{\boldsymbol{\beta}}_1 = \sqrt{\frac{P}{2}}\, \boldsymbol{e}_{max} \tag{65}$$

where $\boldsymbol{e}_{max}$ is the unit-norm eigenvector associated to the maximum eigenvalue of $\mathbf{H}_1$. Taking (57) and (65) into account, it follows that the BER of the optimized scheme is given by

$$\text{BER}_{opt} = Q \left(\sqrt{\frac{1}{2 \cdot \text{SNR}_{opt}^{-1} + N_f T_f B \cdot \text{SNR}_{opt}^{-2}}} \right) \tag{66}$$

where

$$\text{SNR}_{opt} = \frac{N_f \lambda_{max} P}{N_0} \tag{67}$$

λ_{max} being the (maximum) eigenvalue of $\mathbf{H}_1$ associated to $\boldsymbol{e}_{max}$. It is interesting to compare (66) with the BER obtained with a uniform power allocation. In the UPA case, setting $\beta = \sqrt{P/2N_a}$ from (59)–(60) one gets

$$\text{BER}_{UPA} = Q \left(\sqrt{\frac{1}{2 \cdot \text{SNR}_{UPA}^{-1} + N_f T_f B \cdot \text{SNR}_{UPA}^{-2}}} \right) \tag{68}$$

with

$$\text{SNR}_{UPA} = \frac{N_f P \mathbf{1}^T \mathbf{H}_1 \mathbf{1}}{N_a N_0} \tag{69}$$

Compared to UPA, the power gain of the optimum design is given by

$$\frac{\text{SNR}_{opt}}{\text{SNR}_{UPA}} = \frac{\lambda_{max} N_a}{\mathbf{1}^T \mathbf{H}_1 \mathbf{1}} \tag{70}$$

which is greater than or equal to unity since $\lambda_{max} N_a = \lambda_{max} \mathbf{1}^T \mathbf{1} \ge \mathbf{1}^T \mathbf{H}_1 \mathbf{1}$.

In the second case (i.e. the single-antenna scenario), the solution is given by (the proof is omitted)

$$\hat{\beta}_0 = \sqrt{\frac{P}{2}}, \qquad \hat{\beta}_u = \sqrt{\frac{P}{2} \cdot \frac{\varsigma_u}{\varsigma}} \qquad u = 1, 2, \ldots, U \tag{71}$$

where

$$\varsigma_u = 2U \cdot \text{SNR}_{u,opt}^{-1} + N_f T_f B \cdot \text{SNR}_{u,opt}^{-2} \tag{72}$$

$\text{SNR}_{u,opt} = N_f P \mathcal{E}_u / U N_0$, $\mathcal{E}_u$ is the energy of $h^{(u)}(t)$, and $\varsigma = \sum_{u=1}^U \varsigma_u$. As can be seen from (71),

$$\hat{\beta}_0^2 = \sum_{u=1}^U \hat{\beta}_u^2 \tag{73}$$

meaning that, in the single-antenna scenario, the optimal power allocation strategy requires the energy of the reference signal to be equal to the sum of the energies of the information-bearing signals, exactly as it happens in the single-user case. In addition, it can be shown that the bit error rate is the same for all the users, and it is given by

$$\text{BER}_{opt} = Q \left(\sqrt{\frac{U^2}{\varsigma}} \right)$$

$$= Q \left(\sqrt{\frac{U^2}{\sum_{u=1}^U \left[2U \cdot \text{SNR}_{u,opt}^{-1} + N_f T_f B \cdot \text{SNR}_{u,opt}^{-2} \right]}} \right) \tag{74}$$

Now, consider problem (64) for $U \ge 2$ and $N_a \ge 2$. In this case, it can easily be proved the following general result: *The users' BERs, corresponding to the optimal values of the weights, are all the same.* However, the solution cannot be expressed in closed form, and $\mathcal{P}$ can only be solved by resorting to general-purpose optimization tools. Observe, however, that $\mathcal{P}$ (which can easily be casted as the maximization of a linear function subject to quadratic non-convex constraints) is, in general, very difficult to solve (see, for example, [45] and [46]). In order to provide a viable alternative to (63), we consider the following problem:

$$\mathcal{P}': \quad \max_{\boldsymbol{\beta}_0,\ldots,\boldsymbol{\beta}_U} \min_u \quad (\boldsymbol{\beta}_u^T \mathbf{H}_u \boldsymbol{\beta}_0)^2$$

$$\text{subject to} \quad \sum_{u=0}^U \|\boldsymbol{\beta}_u\|^2 \le P \tag{75}$$

which represents a low SNR approximation of $\mathcal{P}$ (it can easily be seen that (63) reduces to (75) in the limit as $N_0 \to +\infty$). By writing the Karush-Kuhn-Tucker (KKT) conditions for problem $\mathcal{P}'$, it is found that its solution has the following form:

$$\hat{\boldsymbol{\beta}}_0 = \sqrt{\frac{P}{2}} \hat{\mathbf{u}}_0, \quad \hat{\boldsymbol{\beta}}_u = \xi_u \mathbf{H}_u \hat{\boldsymbol{\beta}}_0 \qquad u = 1, \ldots, U \tag{76}$$

where

$$\xi_u = \frac{\left(\hat{\mathbf{u}}_0^T \mathbf{H}_u^2 \hat{\mathbf{u}}_0 \right)^{-1}}{\sqrt{\sum_{k=1}^U \left(\hat{\mathbf{u}}_0^T \mathbf{H}_k^2 \hat{\mathbf{u}}_0 \right)^{-1}}} \tag{77}$$

and $\hat{\mathbf{u}}_0$ is the solution of

$$\mathcal{P}'_{eq}: \quad \min_{\mathbf{u}_0} \quad \sum_{k=1}^{U} \left(\mathbf{u}_0^T \mathbf{H}_k^2 \mathbf{u}_0 \right)^{-1} \tag{78}$$
$$\text{subject to} \quad \|\mathbf{u}_0\|^2 = 1$$

Problem $\mathcal{P}'_{eq}$ can straightforwardly be written as

$$\mathcal{P}'_{eq}: \quad \min \quad \sum_{u=1}^{U} y_u^{-1}$$
$$\text{subject to} \quad y_u = \mathbf{u}_0^T \mathbf{H}_u^2 \mathbf{u}_0 \quad u = 1, \ldots, U \tag{79}$$
$$\|\mathbf{u}_0\|^2 = 1$$

which shows that solving $\mathcal{P}'_{eq}$ amounts to minimizing the function $\sum_{u=1}^{U} y_u^{-1}$ over the joint numerical range of the set of matrices $\{\mathbf{H}_1^2, \ldots, \mathbf{H}_U^2\}$. Though the joint numerical range is not always convex, solving $\mathcal{P}'_{eq}$ is clearly much simpler than solving (63).

Vectors (76) represent a good approximation of the solution of (63) at relatively low SNRs. Observe, however, that the users' BERs corresponding to (76) are not expected to be the same for all the users, differently from what happens with the solution of (63). Indeed, with $\hat{\boldsymbol{\beta}}_0$ and $\hat{\boldsymbol{\beta}}_u$ given by (76) we have in general

$$\frac{(\hat{\boldsymbol{\beta}}_{u'}^T \mathbf{H}_{u'} \hat{\boldsymbol{\beta}}_0)^2}{2N_0 \sum_{k=0}^{U} \hat{\boldsymbol{\beta}}_k^T \mathbf{H}_{u'} \hat{\boldsymbol{\beta}}_k + T_f B N_0^2} \neq \frac{(\hat{\boldsymbol{\beta}}_{u''}^T \mathbf{H}_{u''} \hat{\boldsymbol{\beta}}_0)^2}{2N_0 \sum_{k=0}^{U} \hat{\boldsymbol{\beta}}_k^T \mathbf{H}_{u''} \hat{\boldsymbol{\beta}}_k + T_f B N_0^2} \tag{80}$$

for $u' \neq u''$. Accordingly, a better approximation can be obtained as follows. First, we let $\hat{\mathbf{u}}_u$ be the unit-norm vector associated to $\hat{\boldsymbol{\beta}}_u$ as given by (76), i.e.

$$\hat{\mathbf{u}}_u = \frac{1}{\|\hat{\boldsymbol{\beta}}_u\|} \hat{\boldsymbol{\beta}}_u \qquad u = 1, \ldots, U \tag{81}$$

Next, we solve the following *power allocation problem*:

$$\mathcal{P}'': \quad \max_{P_0, \ldots, P_U} \quad t$$
$$\text{subject to} \quad t \leq \frac{\varpi_u P_0 P_u}{2N_0 \sum_{k=0}^{U} \omega_{u,k} P_k + T_f B N_0^2}$$
$$u = 1, \ldots, U$$
$$\sum_{k=0}^{U} P_k \leq P \quad P_k \geq 0 \quad k = 0, \ldots, U \tag{82}$$

with $\varpi_u = (\hat{\mathbf{u}}_u^T \mathbf{H}_u \hat{\mathbf{u}}_0)^2$ and $\omega_{u,k} = \hat{\mathbf{u}}_k^T \mathbf{H}_u \hat{\mathbf{u}}_k$, for $u = 1, \ldots, U$ and $k = 0, \ldots, U$. Finally, denoting by $\hat{P}_0, \hat{P}_1, \ldots, \hat{P}_U$ the solution of (82), we set:

$$\hat{\boldsymbol{\beta}}'_k = \sqrt{\hat{P}_k} \hat{\mathbf{u}}_k \qquad k = 0, \ldots, U \tag{83}$$

and we use (83) instead of (76). By writing the KKT conditions for problem (82), it is found that the constraints must be satisfied with equality, as expected. This means that the solution of $\mathcal{P}''$ together with the maximum value of the objective function are found by solving the following system of equations (in $P_0, \ldots, P_U$ and t):

$$\varpi_u P_0 P_u = t \left(2N_0 \sum_{k=0}^{U} P_k \omega_{k,u} + T_f B N_0^2 \right) \quad u = 1, \ldots, U$$
$$\sum_{k=0}^{U} P_k = P \qquad \sum_{k=1}^{U} \frac{\varpi_k P_k - 2N_0 \omega_{k,0} t}{\varpi_k P_0 - 2N_0 \omega_{k,k} t} = 1 \tag{84}$$

with the constraints

$$P_k \geq 0 \qquad k = 0, \ldots, U \tag{85}$$

In summary, the approximate solution proposed for problem (64) is obtained through the following steps:

s1) The unit-norm vectors $\hat{\mathbf{u}}_k$, for $k = 0, \ldots, U$, are computed by solving problem $\mathcal{P}'$ (which essentially amounts to solving $\mathcal{P}'_{eq}$);

s2) The quantities ϖ_u and $\omega_{u,k}$ are computed for $u = 1, \ldots, U$ and $k = 0, \ldots, U$;

s3) Problem $\mathcal{P}''$ is solved by determining the solution of the system of equations (84) corresponding to the maximum value of t;

s4) Finally, the weighting vectors are fixed according to (83).

It is really worth noticing that, in the single-user case, the sub-optimal procedure provides exactly the same solution of the original problem (64) *at all signal-to noise ratios*.

In order to establish how far the design based on (83) is from the solution of $\mathcal{P}$, we now provide an upper bound to the maximum value of the objective function in (64). To this purpose, we consider the following equation

$$p_0 + t \sum_{u=1}^{U} \frac{2N_0 \lambda_{u,max} p_0 + T_f B N_0^2}{\lambda_{u,max}(\lambda_{u,max} p_0 - 2N_0 t)} = P \tag{86}$$

which implicitly defines the real parameter t as a function of the real parameter p_0. In (86) $\lambda_{u,max}$ is the maximum eigenvalue of $\mathbf{H}_u$, and P is the power constraint in (64). It can be shown (we skip the mathematical details for limitations of space) that the optimal value of (64), say t^*, is upper-bounded by t_{LB}, which is the maximum value of t in (86) when p_0 varies in the interval $[0, P]$. This amounts to saying that the probability of error of the system optimized according to (64), given by $Q(\sqrt{4N_f t^*})$, is lower-bounded by $Q(\sqrt{4N_f t_{LB}})$.

V. SIMULATION RESULTS

Computer simulations have been run to assess the performance of the proposed relaying schemes. The following setting has been adopted. The monocycle $g(t)$ is shaped as the reference pulse of the UWB PHY in the IEEE 802.14.5a standard [47]. It is a root-raised-cosine pulse with a rolloff factor of 0.5, and duration $T_g = 2$ ns. The center frequency of the transmitted signal is $f_c = 3494.4$ MHz with a 3dB bandwidth of 500 MHz (channel #1). The bandwidth of the front-end filter is $B = 1$ GHz. Following [32], the statistics of the propagation channel are taken from the IEEE 802.15.4a model CM2 [48], [49], which corresponds to a residential non-line-of-sight (NLOS) environment. Its rms delay spread is about 13 ns [49]. Parameters T_f and N_f are varied to assess the influence of data rate and IFI. The delays $\tau_n^{(u)}$ in the
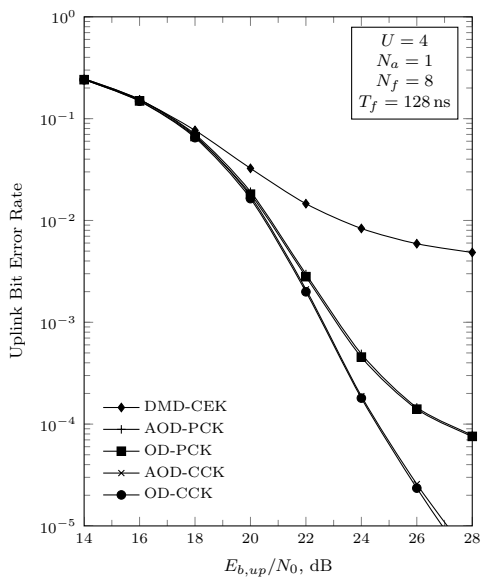
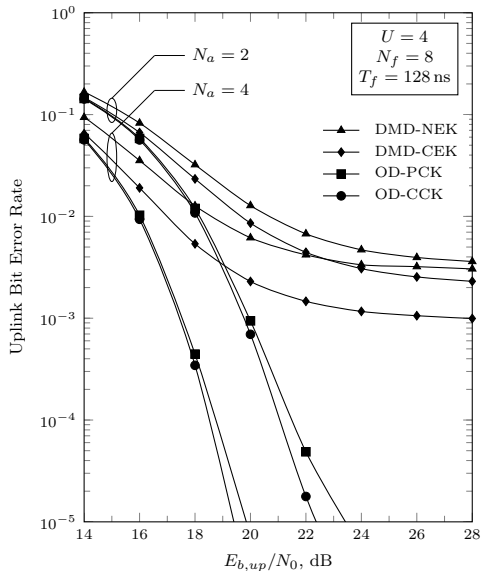Fig. 2: Uplink performance of the proposed relaying schemes with $N_a = 1$, $U = 4$, $N_f = 8$, and $T_f = 128\,\text{ns}$.

Fig. 4: Uplink performance of the proposed relaying schemes with $U = 4$, $N_f = 16$, and $T_f = 64\,\text{ns}$. The number of antennas is $N_a = 2$ or 4.

Fig. 3: Uplink performance of the proposed relaying schemes with $U = 4$, $N_f = 8$, and $T_f = 128\,\text{ns}$. The number of antennas is either $N_a = 2$ or 4.

uplink signal model (6) are modelled as continuous-valued and independent RVs uniformly distributed over a symbol period. Fig. 2 compares the bit error rate performance of the detection schemes in Table I for the source-relay link. The BER curves are plotted as a function of the signal-to-noise ratio (SNR) $E_{b,up}/N_0$, where $E_{b,up}$ is the received energy per bit per user at each antenna. It is understood that $E_{b,up}$ is the same for all users, as would occur when operating under ideal power control conditions. Note that the receiver performance varies from user to user in general, even assuming the same SNR. To account for this fact the numerical values of BER reported in the figure are average values taken over all the users. The number of users is $U = 4$, and the relay has a single antenna, i.e. $N_a = 1$. The number of frames per symbol
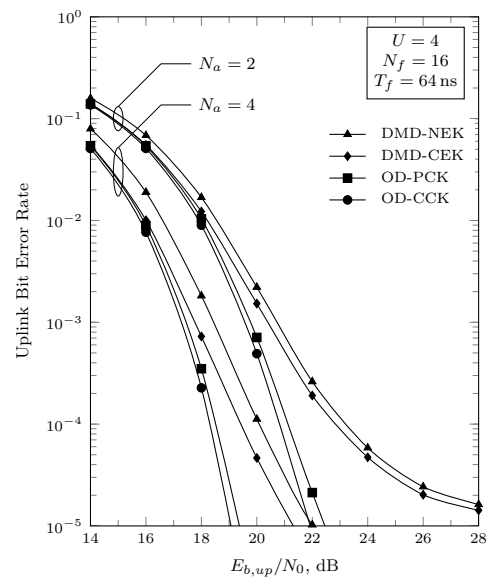
is $N_f = 8$ and the duration of each frame is $T_f = 128\,\text{ns}$. This corresponds to a bit rate $R_b \approx 0.976\,\text{Mbit/s}$ per user. Marks indicate simulation results whereas the thin lines are drawn to ease the reading. It is seen that the optimum detector and the approximate optimum detector (OD and AOD, respectively) have virtually the same performance, with both complete and partial correlations knowledge (CCK and PCK, respectively). The difference between CCK and PCK schemes is negligible for $E_{b,up}/N_0 < 24\,\text{dB}$, but it tends to increase with the signal-to-noise ratio. At $\text{BER} = 10^{-4}$ CCK detectors provide a gain of more than $2\,\text{dB}$ compared to PCK ones. As expected, all these novel detection schemes largely outperform the detector (DMD-CEK curve) proposed in [42]. Notice that DMD-CEK and DMD-NEK have the same performance when $N_a = 1$, and hence the results for DMD-NEK have not been reported in Fig. 2.

Fig. 3 shows the performance of the uplink detection strategies for two different numbers of antennas at the relay, namely $N_a = 2$ (dashed lines) and $N_a = 4$ (solid lines). The other parameters are the same as in Fig. 2. Since OD and AOD schemes have the same performance, only the results for OD-CCK and OD-PCK have been reported. As expected, all the algorithms have improved performance compared to the single-antenna scenario of Fig. 2, but the ranking remains the same. It is worth noticing that the gap between OD-CCK and OD-PCK reduces as N_a increases. On the other hand, the difference between DMD-CEK and DMD-NEK increases with the number of antennas due to a *spatial diversity gain*.

Fig. 4 illustrates BER curves for $N_f = 16$ and $T_f = 64\,\text{ns}$. This means that the number of frames per symbol has doubled compared to the previous figure, while the frame duration has halved. Accordingly, the bit rate is unchanged. The other parameters are the same as in Fig. 3. Contrasting the results of Fig. 4 and Fig. 3, it is seen that all the detection schemes have better performance in passing from $N_f = 8$ to $N_f = 16$. This
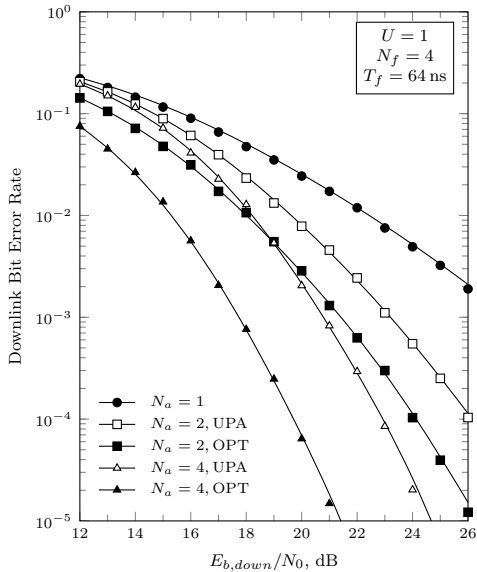
Fig. 5: Downlink performance with UPA and OPT designs, $U = 1$, $N_f = 4$, and $T_f = 64\,\text{ns}$. The number of antennas is $N_a = 1, 2$, or 4.
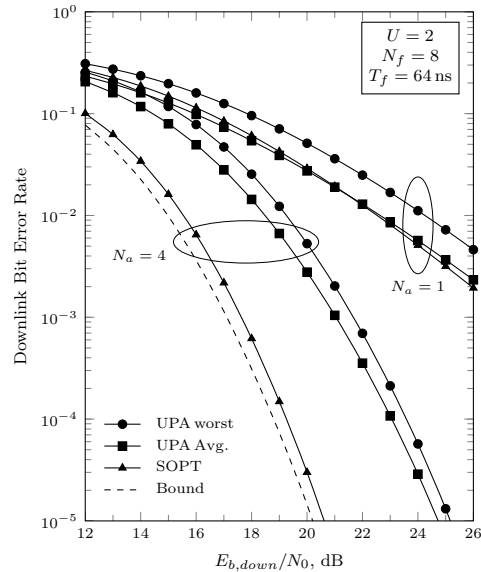

Fig. 6: Downlink performance with UPA and OPT designs, $U = 2$, $N_f = 8$, and $T_f = 64\,\text{ns}$. The number of antennas is $N_a = 1$ or 4.

can be explained by considering that increasing the number of frames (and hence the length of the code sequences) while maintaining T_s fixed improves the robustness against multiple access interference. The detection schemes that mostly benefit from the increment of N_f are those for which rejection of MAI is only left to the cross-correlation properties of the users' codes (i.e. DMD-CEK and DMD-NEK). As a result, the gap between the optimal scheme and DMD reduces significantly, and it becomes less than 2 dB at $\text{BER} = 10^{-4}$. Note, however, that the length of the code sequences cannot be increased arbitrarily while maintaining the same bit rate per user. Indeed, this would amount to decreasing T_f which must be greater than the duration of the overall channel response to prevent IFI. In our case, since the rms delay spread of CM2 is on the order of 13 ns, $T_f = 64\,\text{ns}$ still suffices to avoid IFI.

Now, we consider the BER performance of the downlink transmission schemes discussed in Section IV as a function of the signal-to-noise ratio $E_{b,down}/N_0$, where

$$E_{b,down} = \frac{N_f P}{U N_a} \sum_{n=1}^{N_a} \text{E}\left\{\mathcal{E}_n^{(u)}\right\} \qquad (87)$$

and $\mathcal{E}_n^{(u)}$ is the energy of the channel response $h_n^{(u)}(t)$, between the nth antenna at the relay and the uth receiver. The statistical expectation in (87) is taken with respect to the possible channel realizations. It is easily seen that $E_{b,down}$ is the sum (over the transmit antennas) of the average energies per bit per user at the uth receiver[1]. Note that $E_{b,down}$ may depend on the particular receiver under consideration. Henceforth, for the sake of simplicity it is assumed that $E_{b,down}/N_0$ is the same for all the destination nodes.

Fig. 5 shows the BER performance for the relay-destination

---

[1]Note that $E_{b,down}$ does *not* coincide with the average received energy per bit per user at the uth receiver, because the latter depends on the weights $\boldsymbol{\beta}_v$, for $v = 0, 1, \ldots, U$, differently from the former.

link in a single-user scenario. The number of transmitting antennas is $N_a = 1, 2$, and 4, the number of frames per symbol is $N_f = 4$ and their duration is $T_f = 64\,\text{ns}$. This corresponds to a bit-rate of about $3.9\,\text{Mbit/s}$. Vectors $\boldsymbol{\beta}_0$ and $\boldsymbol{\beta}_1$ are chosen according to either (65) or to the UPA design. Marks (circles, squares, triangles) indicate simulation results while thick lines are theoretical curves obtained by (66) and (68). It is seen that theoretical and measured BERs are in very good agreement. As expected, performance improves with the number of antennas due to a spatial diversity gain. Compared to UPA, the gain of the optimal design given by (70) increases with N_a. For example, at $\text{BER} = 10^{-4}$ it passes from about $2\,\text{dB}$ when $N_a = 2$ to more than $3\,\text{dB}$ for $N_a = 4$. Note that for $N_a = 1$ the optimal and the UPA design provide the same performance (indeed, a single curve is reported in the figure).

In Fig. 6 the performance of the design (83) is compared with that of UPA for $U = 2$. The number of frames per symbol is $N_f = 8$, and $T_f = 64\,\text{ns}$. Accordingly, the aggregate bit-rate is $3.9\,\text{Mbit/s}$, the same as in Fig. 5. The number of antennas is $N_a = 1$ or 4. For each value of N_a three different curves are plotted. The curve with label "UPA Avg." shows the average BER corresponding to the UPA design, the average being taken over all the users (recall that, with the UPA design, the bit error rate may depend on the specific destination node). The curve with label "UPA worst" represents the maximum BER obtained with a uniform power allocation. It provides the benchmark against which the advantages of the sub-optimal design (83) (curve labelled "SOPT") can be measured (indeed, the sub-optimal design *approximately* minimizes the maximum BER. When $N_a = 1$ it has the same performance as the optimal scheme). As can be seen, SOPT outperforms UPA also on average. Its gain increases with the number of antennas. The lower bound obtained through (86) is also reported (curve labelled "Bound") in order to asses how far SOPT could be from the solution of (64). It is seen that, compared to the bound, the loss is a fraction of dB, meaning that the
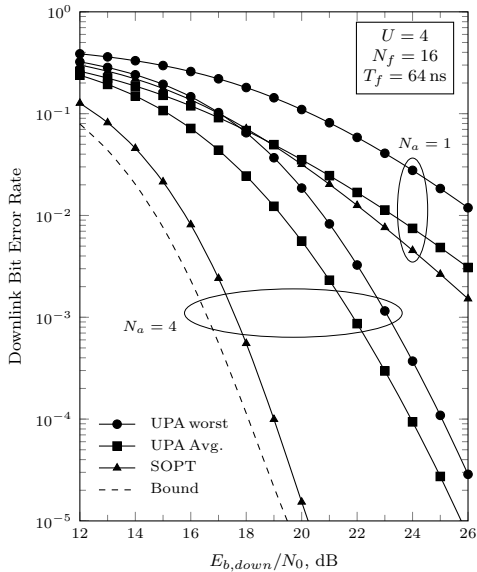
Fig. 7: Downlink performance with UPA and OPT designs, $U = 4$, $N_f = 16$, and $T_f = 64\,\text{ns}$. The number of antennas is $N_a = 1$ or 4.
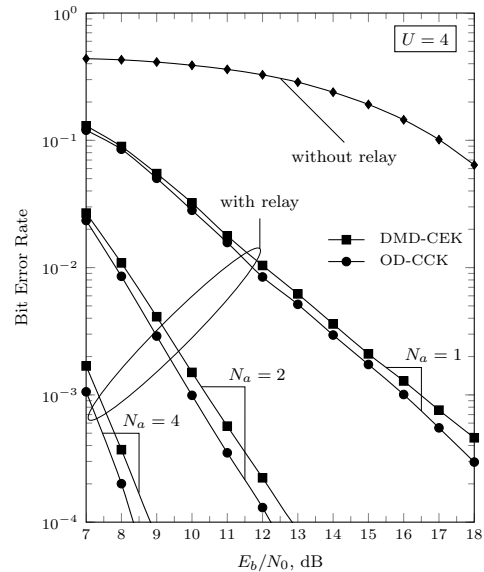

Fig. 8: Comparison between conventional system and relaying schemes (OD-CCK/DMD-CEK in the uplink, optimal weights in the downlink). The number of users is $U = 4$, and $N_a = 1, 2$, or 4.

approximate design provides performance very close to the optimal solution.

The same conclusions hold when the number of users is $U = 4$, as shown in Fig. 7. The number of frames per symbol is $N_f = 16$ while the other parameters are the same as in Fig. 6.

In order to assess the benefit of using the proposed relaying schemes, we consider a network where source and destination nodes are at a distance of d_{SD} meters, whereas the relay is located halfway between them. We ignore the dependence of the pathloss on frequency [48], and we consider only its dependence on the distance between transmitter and receiver. Accordingly, at a given distance d the pathloss in dB is computed as [48]

$$\text{PL}(d) = \text{PL}_0 + 10n \log_{10}\left(\frac{d}{d_0}\right) \qquad (88)$$

where the reference distance d_0 is set to $1\,\text{m}$, PL_0 is the pathloss at the reference distance, and n is the pathloss exponent. Both PL_0 and n depends on the propagation channel. Henceforth, it is assumed that all the considered radio links (namely, between source and destination, source and relay, relay and destination) are statistically described by the channel model CM2, and hence $\text{PL}_0 = 48.7\,\text{dB}$ and $n = 4.58$ [48]. In order to compare conventional and relaying systems fairly, we assume that the total available power is the same in both cases. More precisely, if P_T denotes the power available at each source node in the conventional system (i.e. the system without relay), the same power P_T is evenly split between source and relay in the relaying system. The maximum value of P_T is computed taking into account the limits imposed by FCC [13] on the power spectral density of the transmitted signal ($-41.3\,\text{dBm/MHz}$), while the noise PSD is set at $N_0 = -114\,\text{dBm/MHz}$ (the same value adopted in [27]).

In all the subsequent figures, it is assumed that the vectors $\boldsymbol{\beta}_u$, for $u = 0, 1, \ldots, U$, involved in downlink transmissions,

are obtained through (83). Fig. 8 shows the BER performance of conventional and relaying systems, with $U = 4$, $N_f = 16$, and $T_f = 64\,\text{ns}$. The distance between source and destination nodes is $d_{SD} = 6\,\text{m}$. BER curves are plotted as a function of the signal-to-noise ratio E_b/N_0 at each receiver of the conventional system[2]. Based on the above settings, it is found that the maximum value of E_b/N_0 is about $18.5\,\text{dB}$. A variable number of antennas, namely $N_a = 1, 2$, and 4, is deployed at the relay, and two different detection strategies are considered: OD-CCK (i.e. the best strategy among those listed in Table I, but also the most complex) and DMD-CEK (which has worse performance compared to OD-CCK but much less complexity). Marks indicate simulation results whereas the thin lines are drawn to ease the reading. For the relaying systems the *overall* BER is given by

$$\text{BER} = \text{BER}_{up} + \text{BER}_{down} - 2\text{BER}_{up}\text{BER}_{down} \qquad (89)$$

where BER_{up} is the BER at the relay (for the data transmitted by the source nodes), and BER_{down} is the BER at the destination nodes (for the data transmitted by the relay). As can be seen from Fig. 8, the BER of the conventional system is greater than 10^{-1} at almost all the signal-to-noise ratios. This makes the system without relay useless in many practical applications. On the other hand, using a relay improves the performance dramatically. Note that the two relaying schemes considered in the figure have similar performance, though the performance of OD-CCK are considerably better than that of DMD-CEK (as shown in Figs. 2, 3, and 4). This is explained with the fact that the BER of the relaying schemes is dominated by the BER of downlink transmissions (as can be deduced, for $N_a = 4$, from the results of Fig. 4 and Fig. 7), and hence the choice of the uplink detector has a minor impact

---

[2]Note that fixing E_b for the conventional system amounts to fixing P_T, and hence it amounts to fixing the SNRs at the relay and at the destination nodes in the relaying system.
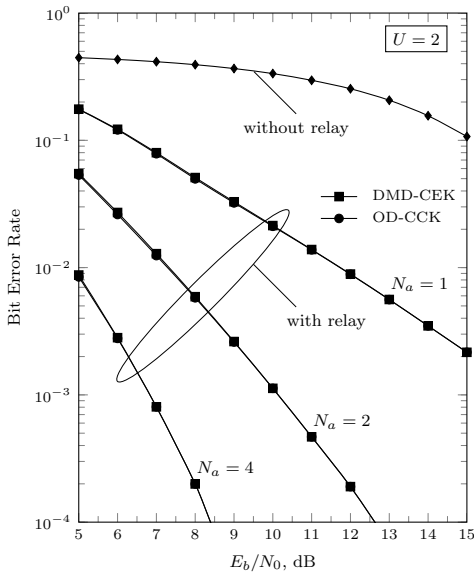
Fig. 9: Comparison between conventional system and relaying schemes (OD-CCK/DMD-CEK in the uplink, optimal weights in the downlink). The number of users is $U = 2$, and $N_a = 1, 2$, or 4.
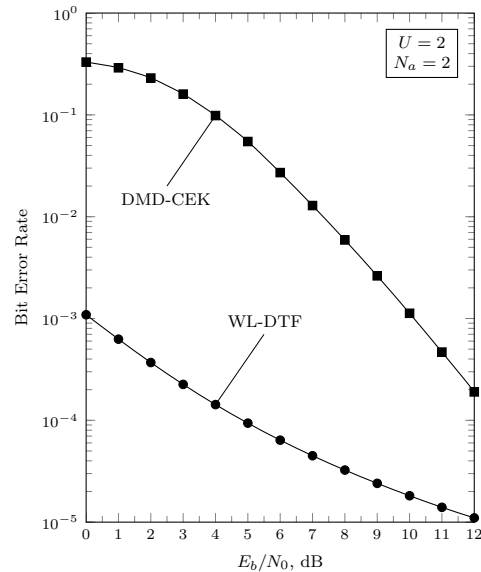

Fig. 10: Comparison between the relaying scheme with DMD-CEK in the uplink and optimal weights in the downlink, and the WL-DFT system proposed in [32, Section II.D]. The number of users is $U = 2$, and $N_a = 2$.

on the overall performance. This would suggest that better performance could be obtained by splitting the total power P_T between source node and relay not evenly (as done here) but in an *optimal* way (see also [27, footnote 2]). This is outside the scope of our paper. The same conclusions are drawn after looking at the results in Fig. 9 where $U = 2$ and $N_f = 8$. The other parameters are the same as in Fig. 8. In this case the maximum value of E_b/N_0 is about 15.5 dB. The curves of the relaying schemes with OD-CCK and DMD-CEK are practically indistinguishable.

Fig. 10 compares the performance of the DMD-CEK based relaying scheme and the Widely Linear DFT system proposed in [32, Section II.D]. The number of antennas is $N_a = 2$ and the other parameters are the same as in Fig. 9. In particular, $T_s = 512$ ns, which guarantees absence of inter-symbol interference in both systems, so that the only impairment is represented by MAI. As expected, the coherent scheme in [32], which is based on (pre/post)-rake filtering, outperforms DMD-CEK (which requires much less channel information and is computationally less demanding) especially at low SNRs. However, it is worth noting that the performance gap tends to reduce as the SNR increases.

The results of Fig. 8 and Fig. 9 have been obtained by assuming a perfect power control. In the conventional system (resp. relaying system) this amounts to saying that at each receiver (resp. relay) the energies (resp. the sum over the receiving antennas of the energies) of the signals of the different users are the same *for each realization* of the prop-agation channels. Different results are obtained by assuming that the above conditions hold not for each realization but *on the average*. This is evident from Fig. 11 which shows the BER performance of conventional and relaying systems as a function of the *average* $\overline{E}_b/N_0$, the average being taken over the channel realizations. The other parameters are the same as in Fig. 8. Compared to Fig. 8, it is seen that both

the conventional system and the relaying schemes have worst performance, as expected. Also, the gap between the relaying system based on OD-CCK and that based on DMD-CEK increases considerably compared to the case of perfect power control.

Finally, Table II compares the coverage of conventional and relaying systems. The coverage is defined as follows: We fix a target bit error rate, say BER_{target}, and compute the maximum distance between source and destination nodes such that BER_{target} is the probability of error when transmissions take place at the maximum power. The path-loss model and the other parameters are the same as in Fig. 8. For the relaying schemes, three different values of coverage are indicated corresponding to $N_a = 1, 2$, and 4, respectively. It is seen that with $N_a = 4$ the coverage of the relaying systems is more than doubled compared to that of a conventional system (approximately the same conclusion holds with $N_a = 2$ as well). The coverage of the relaying schemes with the other uplink detectors of Table I is virtually the same as that with OD-CCK.

TABLE II: Coverage for various network configurations.

Communication system	Uplink detector	Target BER	Coverage
Without relay	——	10^{-2}	5.3 m
Without relay	——	10^{-3}	4.5 m
With relay	OD-CCK	10^{-2}	8.5, 10.2, 11.5 m
With relay	OD-CCK	10^{-3}	6.8, 9.2, 10.7 m

VI. CONCLUSIONS

In this paper we have proposed novel relaying systems for multiuser IR-UWB communications. In order to keep the complexity as low as possible, we have considered non coherent architectures based on code-multiplexing transmitted-reference schemes. Various relaying systems have been pro-posed with different computational complexity and different
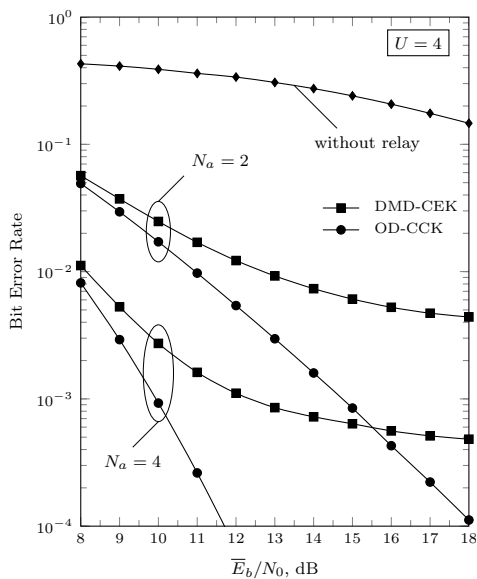
Fig. 11: Comparison between conventional system and relaying schemes with imperfect power control. The number of users is $U = 4$, and $N_a = 2$ or 4.

levels of required channel knowledge. It has been found that even the simplest schemes, with reduced channel state information, largely outperform conventional systems without relay in terms of both bit error rate performance and coverage. The relay-based transceivers mostly benefit from the decode-and-forward protocol, the presence of multiple antennas at the relay, and the higher computational capabilities of the relay compared to the source and destination nodes. Optimizing the power allocation between source nodes and relay could be an interesting topic for further investigation.

A final remark is in order. The proposed schemes are not intended to be used in a system with a high number of users. This means that even the optimal detectors can be implemented with reasonable complexity (in particular OD-PCK). On the other hand, when the number of antennas increases the performance of the low-complexity schemes (in particular DMD-CEK) approaches that of the optimal detector. This means that, with a high number of antennas, DMD-CEK provides a good trade-off between performance and complexity, if the length of the code sequences is sufficiently high to limit the multi-user interference.

References

[1] A. Sibille, "Time-Domain Diversity in Ultra-Wideband MIMO Communications," *EURASIP J. Adv. Sig. Proc.*, vol. 2005, no. 3, pp. 316–327, 2005.

[2] L.-C. Wang, W.-C. Liu, and K.-J. Shieh, "On the Performance of Using Multiple Transmit and Receive Antennas in Pulse-Based Ultrawideband Systems," *IEEE Trans. Wireless Commun.*, vol. 4, no. 6, pp. 2738–2750, June 2005.

[3] S. S. Tan, B. Kannan, and A. Nallanathan, "Performance of UWB Multiple-Access Impulse Radio Systems with Antenna Array in Dense Multipath Environments," *IEEE Trans. Commun.*, vol. 54, no. 6, pp. 966–970, June 2006.

[4] S.-S. Tan, A. Nallanathan, and B. Kannan, "Performance of DS-UWB Multiple-Access Systems with Diversity Reception in Dense Multipath Environments," *IEEE Trans. Veh. Tech.*, vol. 55, no. 4, pp. 1269–1280, April 2006.

[5] C. Abou-Rjeily, N. Daniele, and J.-C. Belfiore, "Space-Time Coding for Multiuser Ultra-Wideband Communications," *IEEE Trans. Commun.*, vol. 54, no. 11, pp. 1960–1972, Nov. 2006.

[6] C. Abou-Rjeily and J.-C. Belfiore, "On Space-Time Coding With Pulse Position and Amplitude Modulations for Time-Hopping Ultra-Wideband Systems," *IEEE Trans. Inf. Theory*, vol. 53, no. 7, pp. 2490–2509, July 2007.

[7] C. Abou-Rjeily and W. Fawaz, "Space-Time Codes for MIMO Ultra-Wideband Communications and MIMO Free-Space Optical Communications with PPM," *IEEE J. Sel. Areas Commun.*, vol. 26, no. 6, pp. 938–947, June 2008.

[8] Q. Zhang and A. Nallanathan, "Delay-Sum Antenna Array Reception for Transmitted-Reference Impulse Radio (TR-IR) Systems," *IEEE Trans. Wireless Commun.*, vol. 7, no. 12, pp. 5208–5213, Dec. 2008.

[9] C. Abou-Rjeily and M. Bkassiny, "Unipolar Space-Time Codes with Reduced Decoding Complexity for TH-UWB with PPM," *IEEE Trans. Wireless Commun.*, vol. 8, no. 10, pp. 5086–5095, Oct. 2009.

[10] T. Kaiser, F. Zheng, and E. Dimitrov, "An Overview of Ultra-Wide-Band Systems with MIMO," *Proceedings of the IEEE*, vol. 97, no. 2, pp. 285–312, Feb. 2009.

[11] H. Nguyen, Z. Zhao, F. Zheng, and T. Kaiser, "Preequalizer design for spatial multiplexing SIMO-UWB TR systems," *IEEE Trans. Veh. Tech.*, vol. 59, no. 8, pp. 3798–3805, Aug. 2010.

[12] A. A. D'Amico, "GLRT-Based Combining Schemes for PPM IR-UWB Systems with Multiple Receive Antennas," *IEEE Trans. Wireless Commun.*, vol. 11, no. 1, pp. 386–396, Jan. 2012.

[13] Federal Communications Commission (FCC), "Revision of Part 15 of the Commissions Rules Regarding Ultra-Wideband Transmission Systems. First Report and Order, ET Docket 98-153," Tech. Rep., 2002.

[14] W. Hirt, "The European UWB Radio Regulatory and Standards Framework: Overview and Implications," in *Ultra-Wideband, 2007. ICUWB 2007. IEEE International Conference on*. IEEE, 2007, pp. 733–738.

[15] T. Kaiser and F. Zheng, *Ultra Wideband Systems with MIMO*. John Wiley & Sons, 2010.

[16] L. Sanguinetti, A. A. D'Amico, and Y. Rong, "A Tutorial on the Optimization of Amplify-and-Forward MIMO Relay Systems," *IEEE J. Sel. Areas Commun.*, vol. 30, no. 8, pp. 1331–1346, August 2012.

[17] G. Kramer, M. Gastpar, and P. Gupta, "Cooperative Strategies and Capacity Theorems for Relay Networks," *IEEE Trans. Inf. Theory*, vol. 51, no. 9, pp. 3037–3063, Sept. 2005.

[18] Z. Wang, T. Lv, H. Gao, and Y. Li, "A Novel Two-Way Relay UWB Network with Joint Non-Coherent Detection in Multipath," in *Vehicular Technology Conference (VTC Spring), 2011 IEEE 73rd*. IEEE, 2011, pp. 1–5.

[19] A. A. D'Amico and U. Mengali, "Code-Multiplexed UWB Transmitted-Reference Radio," *IEEE Trans. Commun.*, vol. 56, no. 12, pp. 2125–2132, December 2008.

[20] C. Abou-Rjeily and A.-R. Marmar, "Novel High-Rate Transmit Diversity Schemes for MIMO IR-UWB and Delay-Tolerant Decode-and-Forward IR-UWB Transmissions," in *Ultra-Wideband, 2009. ICUWB 2009. IEEE International Conference on*. IEEE, 2009, pp. 306–311.

[21] K. Maichalernnukul, T. Kaiser, and F. Zheng, "On the Performance of Coherent and Noncoherent UWB Detection Systems Using a Relay with Multiple Antennas," *IEEE Trans. Wireless Commun.*, vol. 8, no. 7, pp. 3407–3414, 2009.

[22] Y.-L. Chao and R. A. Scholtz, "Ultra-Wideband Transmitted Reference Systems," *IEEE Trans. Veh. Technol.*, vol. 54, no. 5, pp. 1556–1569, May 2005.

[23] A. A. D'Amico and L. Taponecco, "A Differential Receiver for UWB Systems," *IEEE Trans. Wireless Commun.*, vol. 5, no. 7, pp. 1601–1605, May 2006.

[24] M. Hamdi, J. Mietzner, and R. Schober, "Multiple-Differential Encoding for Multi-Hop Amplify-and-Forward IR-UWB Systems," *IEEE Trans. Wireless Commun.*, vol. 10, no. 8, pp. 2577–2591, 2011.

[25] M. Mondelli, Q. Zhou, X. Ma, and V. Lottici, "A Cooperative Approach for Amplify-and-Forward Differential Transmitted Reference IR-UWB Relay Systems," in *Acoustics, Speech and Signal Processing (ICASSP), 2012 IEEE International Conference on*. IEEE, 2012, pp. 2905–2908.

[26] M. Mondelli, Q. Zhou, V. Lottici, and X. Ma, "Joint Power Allocation and Path Selection for Multi-Hop Noncoherent Decode and Forward UWB Communications," *IEEE Trans. Wireless Commun.*, vol. 13, no. 3, pp. 1397–1409, 2014.

[27] Z. Zeinalpour-Yazdi, M. Nasiri-Kenari, and B. Aazhang, "Performance of UWB Linked Relay Network with Time-Reversed Transmission in the Presence of Channel Estimation Error," *IEEE Trans. Wireless Commun.*, vol. 11, no. 8, pp. 2958–2969, Aug. 2012.

[28] T. Strohmer, M. Emami, J. Hansen, G. Papanicolaou, and A. J. Paulraj, "Application of time-reversal with MMSE equalizer to UWB communications," in *Global Telecommunications Conference, 2004. GLOBECOM'04. IEEE*, vol. 5.   IEEE, 2004, pp. 3123–3127.

[29] H. T. Nguyen, J. B. Andersen, and G. F. Pedersen, "The Potential Use of Time Reversal Techniques in Multiple Element Antenna Systems," *IEEE Commun. Lett.*, vol. 9, no. 1, pp. 40–42, Sept. 2005.

[30] H. T. Nguyen, I. Z. Kovács, and P. C. F. Eggers, "A Time Reversal Transmission Approach for Multiuser UWB Communications," *IEEE Trans. Antennas Propag.*, vol. 54, no. 11, pp. 3216–3224, Nov. 2006.

[31] K. Maichalernnukul, F. Zheng, and T. Kaiser, "Design and Performance of Dual-Hop MIMO UWB Transmissions," *IEEE Trans. Veh. Technol.*, vol. 59, no. 6, pp. 2906–2920, 2010.

[32] Z. Ahmadian, L. Lampe, and J. Mietzner, "Multiuser Two-Way Relaying Schemes for UWB Communication," *IEEE Trans. on Wireless Commun.*, vol. 13, no. 11, pp. 6382–6396, Nov. 2014.

[33] C. R. Anderson, S. Venkatesh, J. E. Ibrahim, R. M. Buehrer, and J. H. Reed, "Analysis and Implementation of a Time-Interleaved ADC Array for a Software-Defined UWB Receiver," *IEEE Trans. Veh. Technol.*, vol. 58, no. 8, pp. 4046–4063, Aug. 2009.

[34] R. Hoctor and H. Tomlinson, "Delay-Hopped Transmitted-Reference RF Communications," in *Ultra Wideband Systems and Technologies, 2002. Digest of Papers. 2002 IEEE Conference on*.   IEEE, 2002, pp. 265–269.

[35] A. A. D'Amico and U. Mengali, "GLRT Receivers for UWB Systems," *IEEE Commun. Lett.*, vol. 9, no. 6, pp. 487–489, June 2005.

[36] D. L. Goeckel and Q. Zhang, "Slightly Frequency-Shifted Reference Ultra-Wideband (UWB) Radio," *IEEE Trans. Commun.*, vol. 55, no. 3, pp. 508–519, Mar. 2007.

[37] A. A. D'Amico, "IR-UWB Transmitted-Reference Systems with Partial Channel Knowledge: A Receiver Design Based on the Statistical Invariance Principle," *IEEE Trans. Signal Process.*, vol. 59, no. 4, pp. 1435–1448, April 2011.

[38] M. Weisenhorn and W. Hirt, "Robust Noncoherent Receiver Exploiting UWB Channel Properties," in *Ultra Wideband Systems, 2004. Joint with Conference on Ultrawideband Systems and Technologies. Joint UWBST & IWUWBS. 2004 International Workshop on*.   IEEE, 2004, pp. 156–160.

[39] C. Carbonelli and U. Mengali, "M-PPM Noncoherent Receivers for UWB Applications," *IEEE Trans. Wireless Commun.*, vol. 5, no. 8, pp. 2285–2294, Aug. 2006.

[40] A. A. D'Amico, U. Mengali, and E. Arias-de Reyna, "Energy-Detection UWB Receivers with Multiple Energy Measurements," *IEEE Trans. Wireless Commun.*, vol. 6, no. 7, pp. 2652–2659, July 2007.

[41] A. A. D'Amico and U. Mengali, "Multiuser UWB Communication Systems with Code-Multiplexed Transmitted Reference," in *Communications, 2008. ICC'08. IEEE International Conference on*.   IEEE, 2008, pp. 3765–3769.

[42] ——, "Code-Multiplexed Transmitted-Reference UWB Systems in a Multi-User Environment," *IEEE Trans. Commun.*, vol. 58, no. 3, pp. 966–974, March 2010.

[43] H. Urkowitz, "Energy Detection of Unknown Deterministic Signals," *Proceedings of the IEEE*, vol. 55, no. 4, pp. 523–531, 1967.

[44] D. P. Palomar and Y. Jiang, "MIMO Transceiver Design Via Majorization Theory," *Foundations and trends in communications and information theory*, vol. 3, no. 4, pp. 331–551, 2006.

[45] F. A. Al-Khayyal, R. Horst, and P. M. Pardalos, "Global optimization of concave functions subject to separable quadratic constraints and of all-quadratic separable problems," Production and Distribution Research Center, Georgia Institute of Technology, Atlanta, Report Series No. PDRC 88-04, 1988.

[46] C. A. Floudas and V. Visweswaran, "Quadratic Optimization," in *Handbook of Global Optimization*.   Springer, 1995, pp. 217–269.

[47] IEEE Standard 802.15.4a Task Group, "Part 15.4: Low-Rate Wireless Personal Area Networks (LR-WPANs)," IEEE Computer Society, Tech. Rep., 2011.

[48] A. F. Molisch, D. Cassioli, C.-C. Chong, S. Emami, A. Fort, B. Kannan, J. Karedal, J. Kunisch, H. G. Schantz, K. Siwiak *et al.*, "A Comprehensive Standardized Model for Ultrawideband Propagation Channels," *IEEE Trans. Antennas Propag.*, vol. 54, no. 11, pp. 3151–3166, Nov. 2006.

[49] A. F. Molisch, K. Balakrishnan, D. Cassioli, C.-C. Chong, S. Emami, A. Fort, J. Karedal, J. Kunisch, H. Schantz, U. Schuster *et al.*, "IEEE 802.15. 4a Channel Model - Final Report," *IEEE P802*, 2004.